Feasibility Study of an Airbag-Based Crew Impact Attenuation System for the Orion MPCV

Sydney Do* and Olivier de Weck†
Department of Aeronautics and Astronautics, Massachusetts Institute of Technology, Cambridge, MA, 02139

Airbag-based methods for crew impact attenuation have been highlighted as a potential lightweight means of enabling safe land-landings for the Orion Multi-Purpose Crew Vehicle, and the next generation of ballistic shaped spacecraft. To investigate the performance feasibility of this concept during a nominal 7.62m/s Orion landing, a full-scale personal airbag system 24% lighter than the Orion baseline has been developed, and subjected to 38 drop tests on land. Through this effort, the system has demonstrated the ability to maintain the risk of injury to an occupant during a 7.85m/s, 0° impact angle land-landing to within the NASA specified limit of 0.5%. In accomplishing this, the airbag-based crew impact attenuation concept has been proven to be feasible. Moreover, the obtained test results suggest that by implementing anti-bottoming airbags to prevent direct contact between the system and the landing surface, the system performance during landings with 0° impact angles can be further improved, by at least a factor of two. Additionally, a series of drop tests from the nominal Orion impact angle of 30° indicated that severe injury risk levels would be sustained beyond impact velocities of 5m/s. This is a result of the differential stroking of the airbags within the system causing a shearing effect between the occupant seat structure and the spacecraft floor, removing significant stroke from the airbags.

I. Introduction

Since the start of its development in late 2006, the Orion Multi-Purpose Crew Vehicle (then named the Orion Crew Exploration Vehicle) has experienced several modifications to its operational and design architecture as trade studies have been completed and more knowledge about the system obtained. One prevalent aspect regularly revisited throughout the program is the baseline mode in which the vehicle is to land on the Earth's surface, and consequently the concept which should be employed to facilitate this landing. This uncertainty has been linked to a combination of a strained mass budget, and difficulties in developing systems capable of protecting astronauts during all possible landing scenarios[1]. This paper presents the work that was conducted in an attempt to provide further insight into this problem, by evaluating the feasibility of implementing an alternative, lightweight, airbag-based crew impact attenuation system within the cabin of the Orion Crew Module in order to facilitate safe land-landings. This was achieved through the complete design, development, and drop testing of a full-scale personal airbag system. This work forms one component of a greater study conducted by the NASA Engineering and Safety Center (NESC) team to provide design recommendations for the Orion landing system architecture. Specifically, the results of this work will be used by the NESC to decide whether or not to further pursue airbag-based crew impact attenuation for both current and future versions of Orion, and for future crewed spacecraft.

II. Background and Motivation

It is an interesting fact that every capsule-shaped reentry vehicle developed by NASA initially had a specific requirement to land on land, but was ultimately designed to land in water, due to the technical and schedule risks involved. With the schedule pressures of the Cold War space race long gone and the desire to develop a sustainable, long-term space transportation program; there was an interest in revisiting the possibility of developing a land-landing capability for Orion from the outset.

* Graduate Research Assistant, Department of Aeronautics and Astronautics, Massachusetts Institute of Technology, Cambridge, MA, 02139, and AIAA Student Member.
† Associate Professor, Department of Aeronautics and Astronautics & Engineering Systems Division, Massachusetts Institute of Technology, Cambridge, MA, 02139, and AIAA Associate Fellow.

Inherently more challenging than the traditional "splashdown" mode, this ever-present desire for land-landing arises primarily from considerations related to the recovery and refurbishment of the vehicle. Recovering a vehicle from sea is inherently more challenging than recovering one from land. This is due to the added difficulty in gaining access to a target moving in a dynamic marine environment, as well as the need to keep the vehicle afloat to prevent flooding[2]. Contrastingly, land-landings facilitate easier egress and recovery of the vehicle, while also mitigating the risk of water damage. This latter attribute has implications on the ease of refurbishment and reusability of the spacecraft, which in turn impacts on the life-cycle costs of the program[1] – a particularly important factor in the current era of human spaceflight commercialization. The disadvantage of employing a land-landing mode, however, is that the increased hardness of the landing surface results in higher accelerations being imparted upon the crew during impact. This hence requires a more complex, and inevitably higher mass system.

During a preliminary study conducted by the NESC in early 2007, the risks and costs involved in land versus water landings for Orion were accessed[2]. From this, it was concluded that the operational and life-cycle benefits of nominal land-landings far offset their inherent additional complexity, resulting in a recommendation for the Orion CEV to adopt a primary land-landing mode. To support this development, the NESC further recommended that a study be conducted to investigate various options for further injury-risk mitigation during land-landings. Here, a specific mention was made to:

"*Pursue an alternate approach to the internal astronaut couch attenuation system based on difficult experience with [the] Apollo strut support system. The current CEV design of the astronaut couch and associated couch attenuation system should be revisited"* (Ref. 2)

To address this recommendation, a workshop was conducted by the NESC in the summer of 2008, where a team of academic and industry experts were tasked to develop alternative concepts to this couch-based attenuation system design. Moreover, prior to this workshop, a decision was made for Orion to revert back to a nominal water-landing mode in an attempt to bring the vehicle back to within its mass allocation, thus motivating the need for the developed concepts to be lightweight. As a result, the idea of the personal airbag system was born.

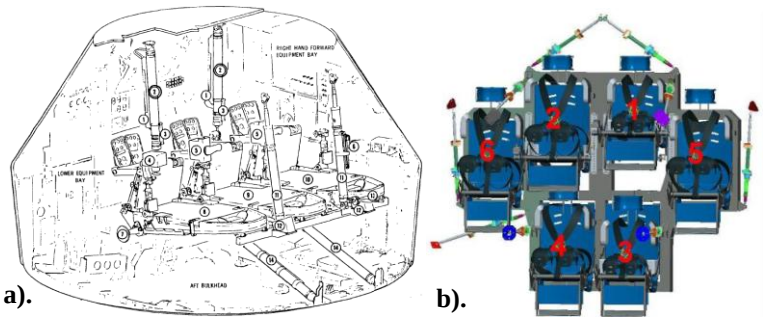

Figure 1. Comparison of Apollo and baseline Orion Crew Impact Attenuation Systems used to protect astronauts from the impact loads incurred during landing. Both systems are based on the same concept of a rigid pallet carrying crew seats, supported by a rigid pallet a). Apollo[3] b). Current Orion Baseline[1]

Inspired from the structure of seeds in nature, this concept involves using an inflated airbag "seat" to protect the occupant during landings of the Orion crew module. Just as seeds protect their embryos from mechanical loads by surrounding them with a layer of endosperm, this concept involves surrounding the astronaut in a personal cushion of air. When crew positioning requirements were factored, this concept evolved into the personal airbag system. The original ideation process used to develop this concept is shown below in Figure 2.

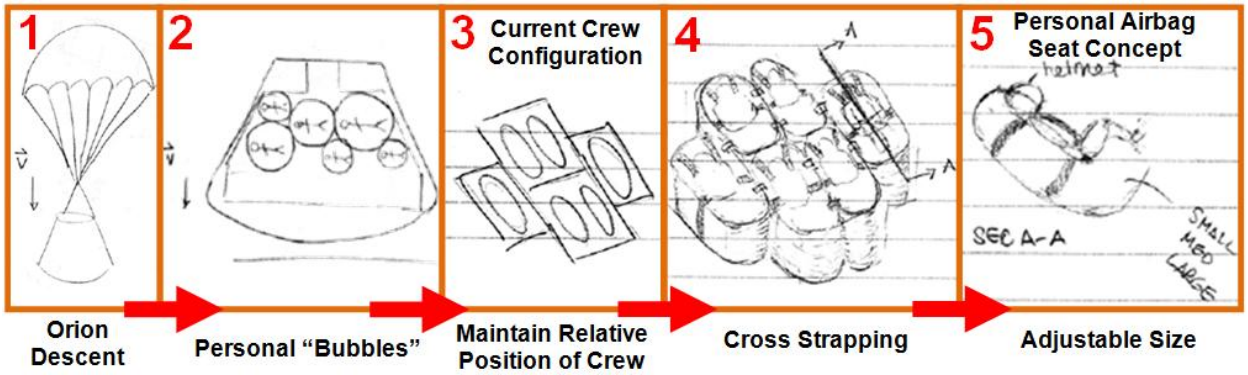

Figure 2. Original Ideation Process used to Conceptualize the Personal Airbag System

In addition to being inherently lightweight, this system has the advantage of being able to be deflated and stowed when not in use, thus providing additional in-cabin volume. Initial estimates have found that these savings equate to a potential 36% reduction in the mass without the crew, and an increase in 26% of in-orbit habitable volume[4], when compared to the baseline Orion system. From an operational viewpoint, this latter attribute is particularly beneficial when the spacecraft is in orbit and seats are no longer required. This is demonstrated in the system concept of operations, depicted in Figure 3.

Thus, in an effort to further develop this concept and investigate its land-landing crew impact attenuation potential; a full-scale personal airbag system was designed, fabricated, and subjected to a series of drop tests. The following sections describe the efforts that led to the development of this system, the results obtained from the rigorous test campaign undertaken, and the implications of these results on the feasibility of implementing such a system aboard the Orion vehicle.

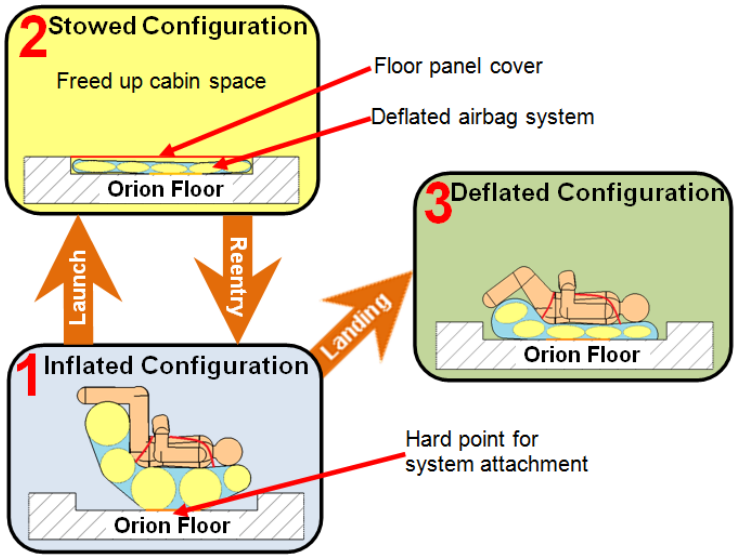

Figure 3. System Concept of Operations consisting of the Inflated, Stowed, and Deflated Configurations. During pre-launch and launch, the system would be in the Inflated state to function as a seat to support the occupant. Once in space, the system would transition to the Stowed state to increase available cabin space. Prior to reentry, the system is then returned to its Inflated state in preparation for landing. Upon landing, the seat transitions to the Deflated state as it attenuates the impact loads subjected to the crew.

III. Development Approach

In order to investigate the potential of airbag-based crew impact attenuation for facilitating safe land-landings, a three-level spiral model of system development was employed. This involved cycling through the complete development process, from system conception through to its detailed design, implementation, and operation, three times. In each subsequent cycle, lessons learned from the previous were used to develop an improved next generation of the system.

Specifically, the first spiral focused on developing and testing a complete analog airbag system. Here, an analog version of the system was chosen to facilitate a quick collection of experience and knowledge under relaxed design requirements. Through this effort, insights into the relative positioning of the airbags with respect to the occupant support structure, as well as the system failure modes were obtained. The development and testing of this system, as well as the lessons learned and insights gained from this effort are extensively described in Ref. 5.

From these lessons learned, a single airbag drop test article was developed in the second spiral. Here, the primary objective was to develop an understanding of the impact dynamics of a single airbag through a series of characterization drop tests. The results of these tests were then used to validate impact models

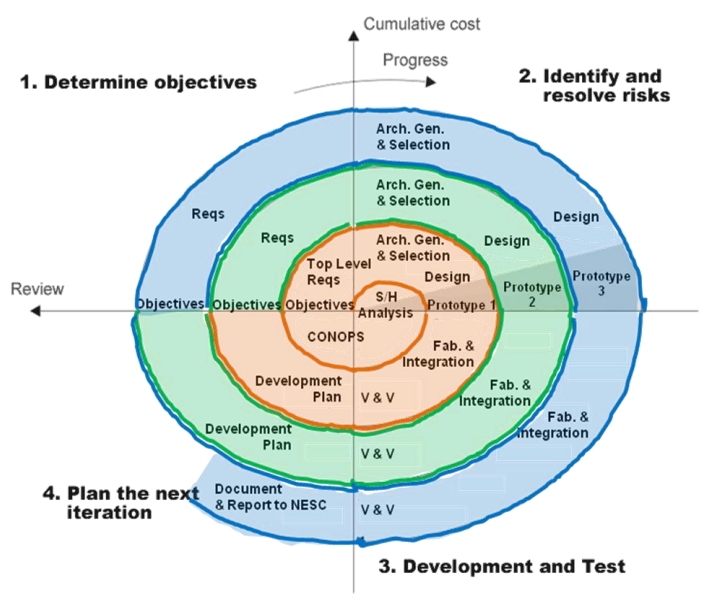

Figure 4. Three Level Spiral Model used for this Development Effort (Adapted from Ref. 6)

created to design the system (see Section IV). In addition, this second spiral led to the in-house development, testing, and validation of flapper valves, as well as the determination of airbag manufacturing techniques, including airbag stitch patterns, and treatment methods for fabric leakproofing (See Ref. 7 for details).

Using the experience and data gained from the first two development spirals, a full-scale personal airbag system was then developed and subjected to a series of drop tests in the final spiral, thus allowing for the feasibility of the airbag-based crew impact attenuation system concept to be determined. The approach used to develop and test this final system, as well as the test results obtained and their analysis, will be described in the subsequent sections.

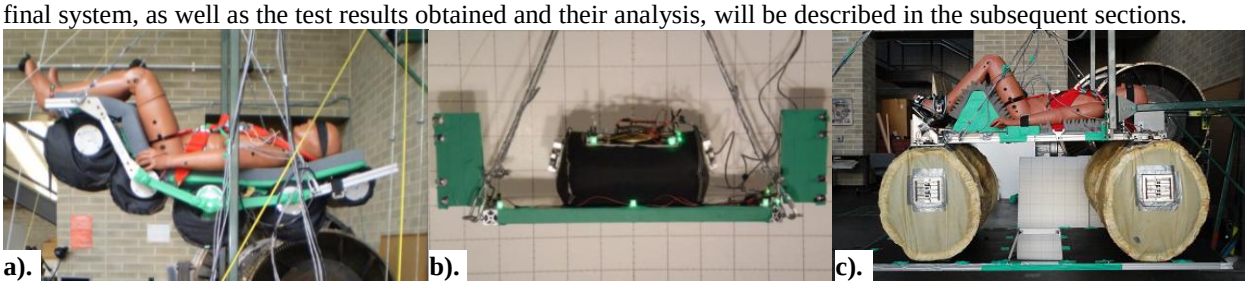

Figure 5. Drop Test Articles Developed for each Spiral of System Development a). Analog Airbag System b). Single Airbag Drop Test Article c). Personal Airbag System

IV. System Modeling

As was conducted throughout all development spirals, the development of the full-scale personal airbag system consisted of firstly developing a baseline airbag configuration based upon knowledge obtained from previous design spirals; followed by optimizing the size of the individual airbags such that the injury risk subjected to the occupant was minimized. In order to achieve this, both an airbag impact model, and a means of quantifying injury risk are required. The tools developed to fulfill these needs are described below.

A. The Brinkley Direct Response Index

To ensure a common framework for measuring injury-risk to astronauts during transient acceleration environments, NASA has mandated that the Brinkley Direct Response Index (DRI) be used in the design and development of all human spacecraft crew impact attenuation systems[8]. This index measures the risk of injury to an occupant given a measured acceleration profile by comparing the output of a dynamics model of the human body, to limiting values representing varying levels injury-risk (Table 2). In order for a system to be considered safe, the maximum Brinkley DRI experienced during an acceleration event must remain within the "low" injury-risk bounds, which equates to a 0.5% likelihood of injury sustained anywhere on the body.

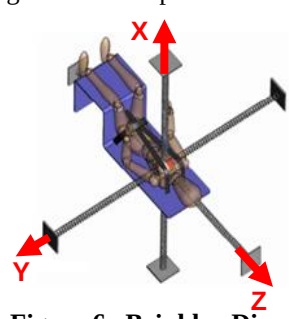

Figure 6. Brinkley Direct Response Index Model[9]

With regard to the dynamics model used to determine the Brinkley DRI, a lumped parameter model is utilized. This model approximates the dynamic response of a human as that of a spring-mass-damper system to a given acceleration profile in each of the three orthogonal axes, referenced to the center of the torso. A simplifying assumption made is that the effects of the applied acceleration profile in each of the three axes are decoupled. This dynamic system is modeled with the following relationship:

$$\ddot{X}(t) + 2\xi\omega_n \dot{X}(t) + \omega_n^2 X(t) = A(t) \tag{1}$$

Where:

X is the relative displacement coordinate of the of the dynamic system with respect to the center of the torso in either one of the x-, y-, or z-directions. Here, a positive value corresponds to a compression

A is the measured acceleration profile from the reference point in either one of the x-, y-, or z-directions

ξ is the damping ratio of the dynamic system representing the response in the given x-, y-, or z-direction

ω_n is the natural frequency of the dynamic system representing the response in the given x-, y-, or z-direction; and

t is a time coordinate

The Brinkley DRI is obtained by solving the system given by Eq. (1) and inputting the result into the following relationship:

$$DRI(t) = \frac{\omega_n^2 X(t)}{g} \tag{2}$$

Where g is the acceleration due to the Earth's gravity, used here as a normalizing factor. Furthermore, the damping ratio and natural frequency values to be used in the aforementioned lumped parameter model as specified by the NASA HSIR are as follows:

Table 1 – NASA HSIR specified natural frequencies and damping ratios to be used in the Brinkley Dynamic Response Model (Ref. 8)

	x	*y*	*z*
ω_n	62.8	58.0	52.9
ξ	0.2	0.09	0.224

Table 2 – NASA HSIR Specified Brinkley DRI Limits (Ref. 8, 9)

	x		***y***		***z***	
Brinkley DRI Limit Level	**$DRI_x < 0$**	**$DRI_x > 0$**	**$DRI_y < 0$**	**$DRI_y > 0$**	**$DRI_z < 0$**	**$DRI_z > 0$**
Very Low (0.05%)	-22.4	31	-11.8	11.8	-11	13.1
Low (0.5% - Safe Limit)	-28	35	-14	14	-13.4	15.2
Moderate (5%)	-35	40	-20	17	-12	18
High (50%)	-46	46	-30	22	-15	22.8

Note that the percentage values listed next to the Brinkley DRI limit levels correspond to the likelihood of injury to the occupant at any location on the body.

Since the DRI is a time-dependent function, a parameter called the β-function is commonly used to determine if a system has remained below a given Brinkley limit over the duration of an acceleration event. As shown in Eq. 3, this function corresponds to the root sum square of the relative DRI values in each of the three orthogonal axes.

$$\max\{\beta\} = \max\left\{\sqrt{\left(\frac{DR_x(t)}{DR_x^{\lim}}\right)^2 + \left(\frac{DR_y(t)}{DR_y^{\lim}}\right)^2 + \left(\frac{DR_z(t)}{DR_z^{\lim}}\right)^2}\right\} < 1 \tag{3}$$

Here, a maximum beta value of less than one corresponds to the system satisfying a given injury-risk level over the duration of an impacting event.

B. Single Airbag Model

Fundamentally, airbags attenuate impact loads by converting the kinetic energy of an impacting object into the potential energy of the airbag gas, as the object does boundary work on the airbag. This energy is then removed from the system by venting the gas at predefined conditions. Depending on the amount of gas vented, the system will either experience a bounce after the initial impact or come to an immediate rest. In this regard, airbags can be considered as non-linear springs, whose stiffness is dependent on the geometry of the airbag (which in turn influences the boundary work done by the supported object on the airbag gas); and the venting characteristics of the airbag (which subsequently dictates the amount of gas and hence energy released from the airbag, and the period of time and duration at which this occurs). This can be seen when performing a force balance on an idealized airbag supporting a payload mass, as depicted in Fig, 7.

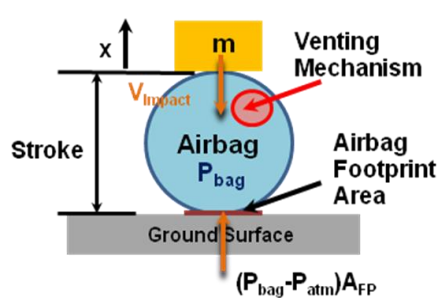

Figure 7. Idealized Single Airbag Impact Case

Here, it can be observed that the forces present in this single degree of freedom model are:

- The force resulting from the acceleration of the mass sitting atop the airbag as it impacts with the ground surface
- The weight force of the mass sitting atop the airbag; and
- The reaction force from the ground surface, which can be simplified to be equivalent to the effects of the differential pressure between the airbag operating medium and the local atmosphere on the contacting area

Performing a force equilibrium with these forces in the vertical direction yields the following system equation:

$$\overbrace{m\ddot{x}}^{Acceleration} + \overbrace{\left(P_{bag}(x) - P_{atm}\right)A_{FP}(x)}^{Reaction\ Force} = \overbrace{mg}^{Weight} \tag{4}$$

Here, it can be observed that this equation is in the form of a mass-spring system, with a nonlinear spring stiffness, given by:

$$k(x) = \frac{1}{x(t)}\left(P_{bag}(x,t) - P_{atm}\right)A_{FP}(x) \tag{5}$$

Observing Eq. (5), it can be seen that it is the interaction between the airbag pressure and its geometry which causes the nonlinearity of the airbag stiffness. When the combination of these variables is appropriately chosen, it is this nonlinearity which yields the damping effectively experienced by the payload mass during impact. In order to determine the values of these variables, a framework based on the original dynamics model used to develop the airbag system for the Mars Pathfinder[10] was implemented. Specifically, this framework treats the airbag impact attenuation problem from a fluid mechanics perspective, using an Euler time stepping scheme to determine the change in airbag geometry based on the vertical position of the supported mass at each time increment. This geometry solution is then used to obtain the pressure, volume, and mass of the operating medium, which is in turn used to determine conditions for venting of the airbag. It should be noted here that for the entire personal airbag system development, the baseline airbag geometry was limited to be that of the cylinder. This was chosen primarily for the purposes of manufacturability. Figure 8 presents a top level N^2 diagram of the model.

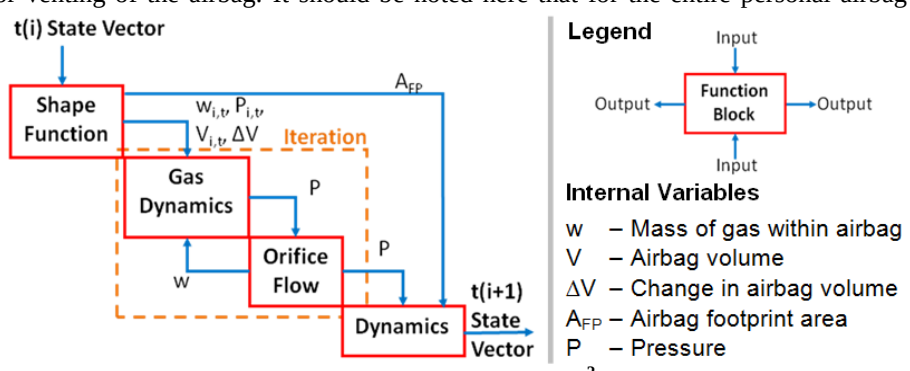

Figure 8. Single Airbag Impact Model Top Level N^2 Diagram

To model the geometry of the airbag, two shape functions were implemented to represent its changing volume and ground contact surface during its compression. Based on those used by Esgar and Morgan[11], these shape functions assume that the axial length of the cylindrical airbags remains constant throughout the compression process. As a result, these functions only focus on the changing cross section of the airbag from its initial circular shape (see Fig. 9).

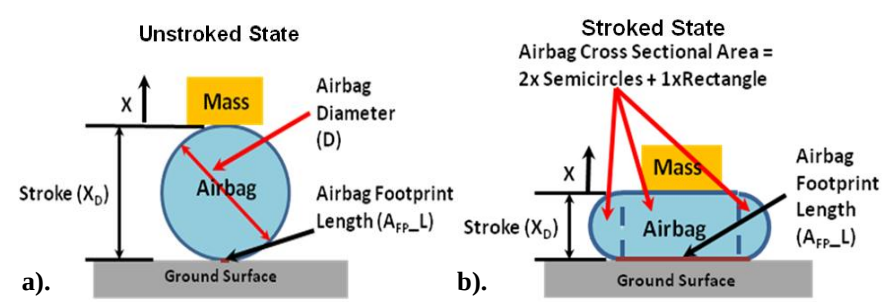

Figure 9. Shape Functions used in the Single Airbag Impact Model a). Unstroked State b). Stroked State

To accomplish this, a condition is enforced such that the circumference of the airbag cross section remains constant. In effect, this is equivalent to a conservation of airbag surface area condition. Hence, in terms of the framework presented in Fig. 9b)., this can be expressed as:

$$\text{Unstroked Airbag Circumference} = \text{Stroked Airbag Circumference} \tag{6}$$

Enforcing this condition and taking advantage of the simplified stroked state geometry shown in Fig. 9b), the following relationships for airbag footprint area and airbag volume as a function of stroke can be derived:

$$\text{Airbag Footprint Area}: A_{FP}(X_D) = L\pi(D - X_D)$$
$$\text{Airbag Volume}: V(x) = LX_D\left(\frac{\pi X_D}{4} + A_{FP} - L\right) \tag{7}$$

Where L is the fixed airbag axial length.

Here, the simplifying approach of using geometric shape functions was chosen over more computationally intensive fluid structure interaction methods due to the latter's inherently long computation times. Because the objective at this design level was to develop a general understanding of the effects of the design variables on the overall system performance, it was deemed that the benefits of quick lower fidelity function evaluations far outweighed any benefits of a higher fidelity model which took vastly longer to execute. This was particular so due to the ability of computationally inexpensive models to generate complete design spaces over a relatively short evaluation time. These design spaces in turn allowed for the sensitivity of the system performance to the design variables to be investigated in an efficient manner.

In regards to the gas dynamics and orifice flow equations, a simplifying assumption is made whereby the operating medium is treated as an ideal gas, and that the impact attenuation process is one which is isentropic. Because the airbag operating medium was fixed to be atmospheric air (for ease of testing and operations purposes), the ideal gas assumption is valid. Moreover, the isentropic process assumption is widely used to model typical engineering devices such as pumps, nozzles, and turbines, which operate in an essentially adiabatic manner[12]. Since the airbag impact attenuation process is also essentially adiabatic, and because the impact of irreversible effects is relatively small; the isentropic process assumption is appropriate. The specific equations used, and their interactions with each other, are summarized in the functional flow block diagram below. Note that a full derivation of all equations used to develop this model is provided in Refs. 7 and 10.

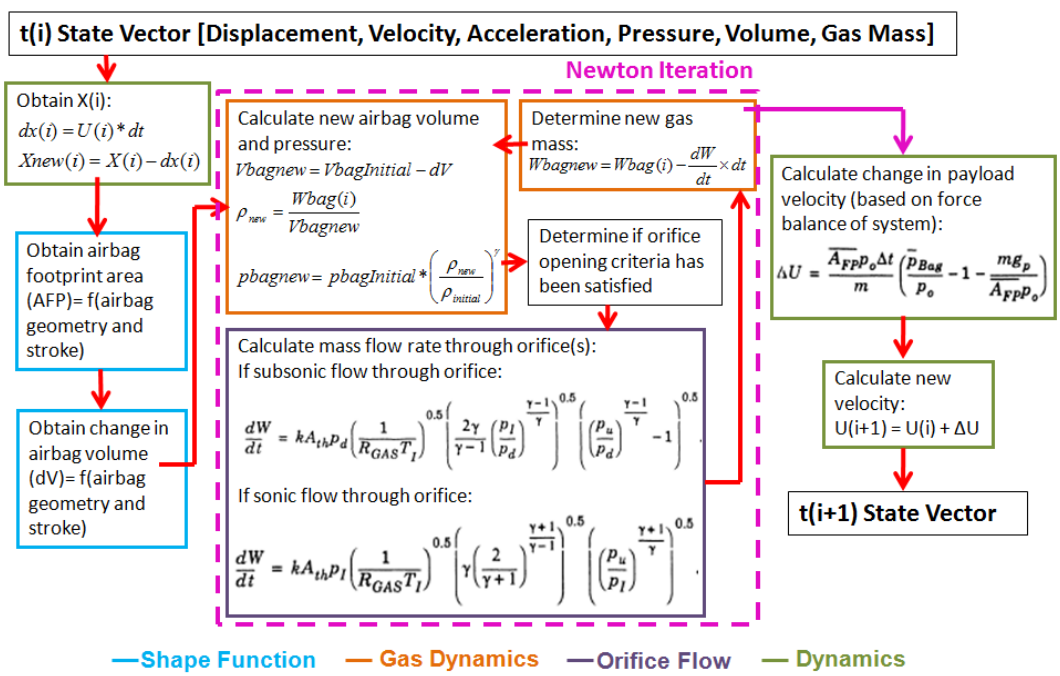

Figure 10. Single Airbag Impact Model Functional Flow Block Diagram

Additionally, in order to obtain the injury-risk response of the supported payload during a given impact event, the acceleration response obtained from executing the single airbag model is input as the forcing function into Eq. (1). From this, the Brinkley DRI is obtained and compared to the limits given in Table 2, thereby yielding the injury-risk subjected to the occupant.

C. Single Airbag Model Validation

As was mentioned in Section III, one of the objectives of the second spiral of system development was to validate the predictions made by the single airbag model. This was successfully achieved by using the single airbag

drop test campaign results to refine the airbag shape function and airbag venting characteristics. This can be seen in the comparison between the experimentally-obtained and model-predicted acceleration responses presented below. Here, drop tests were performed at varying drop heights to characterize the system dynamics at different impact velocities. Specifically, three drops were performed at each drop height, as indicated in the legend of Fig. 11a).

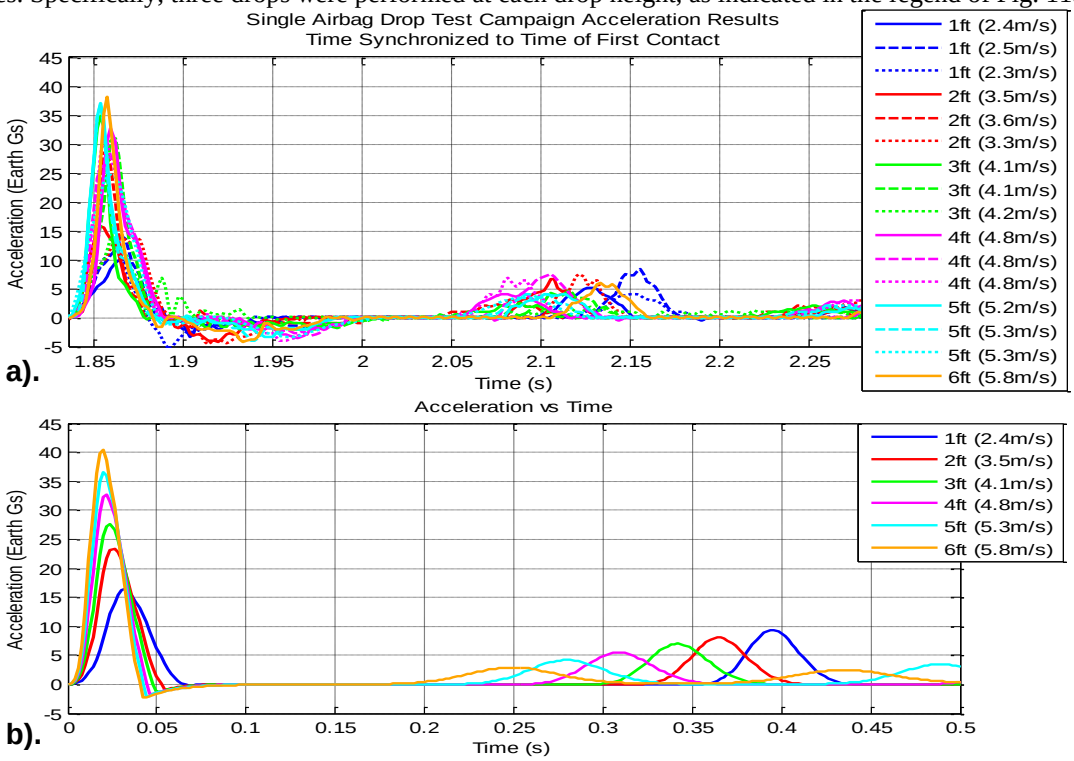

Figure 11. Comparison between Experimentally-Obtained, and Model-Predicted Acceleration Profiles a). Experimentally obtained data b). Model prediction

From Fig. 11, it can be seen that for all drop tests, the model over-predicts, the peak acceleration by at most 2Gs. This is a favorable result from a design perspective due to its slight conservatism.

D. Design Space Exploration

In addition to validating the single airbag impact model, a separate study was performed to gain insight into the effects of the airbag geometry, inflation, and venting characteristics on the overall system performance. This involved performing a full factorial expansion of the design space for a system with a fixed payload mass, and analyzing the results from both the single and multi-objective standpoints. Specifically, the objectives were to minimize the peak Brinkley DRI, and to minimize the overall system mass. Two key findings were made during this exercise, being:

- *For a fixed airbag geometry, the Brinkley response is most sensitive to changes in the venting area*

This can be explained by considering the energy exchanges which occurs during the impact process. Fundamentally, the venting area dictates the amount and rate at which gas is vented from the airbag, which in turn, equates to the amount of energy being removed from the system

- *For a system using pressure relief valves as the primary venting mechanism, the mass and injury-risk optimal design is one with the minimum airbag geometry such that bottoming-out (that is, direct contact between the payload mass and the impacting surface) does not occur.*

This finding arises from the unintuitive observation that systems with lower peak Brinkley DRI values tended to have smaller geometries. This is because under the same impact conditions, smaller airbags are able to maintain a higher pressure over a longer period of time, causing the pressure relief valves to remain open for a longer period of time. This effectively increases the cumulative venting area when integrated over the impact duration, thereby allowing more gas to exit the system and leading to improved impact attenuation. The lower bound on this geometry

occurs when there is insufficient stroke to remove all kinetic energy from the payload mass prior to it directly impacting the landing surface. This can be seen in the objective space shown below.

Here, it can be seen that a Pareto front of non-dominated designs exists in the system mass versus Brinkley DRI objective space. Moreover, moving along this Pareto front corresponds to varying the valve burst pressure at the minimum airbag geometry such that bottoming-out does not occur. It is this bottoming-out limit which causes the Pareto front to exhibit a concave shape, due to the fact that before reaching this limit, the objectives of minimizing both system mass and injury-risk are mutually supportive.

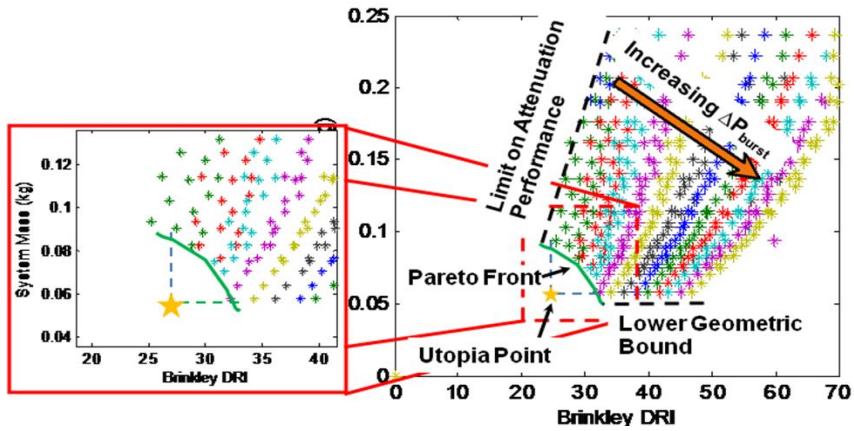

Figure 12. Full Factorial Expansion of the Objective Space. Points of the same color correspond to those with the same valve opening pressure

E. Multi-Airbag Modeling

With a validated single airbag impact model established, a multi-airbag impact model was developed to facilitate the design of the personal airbag system. This model exploits the non-linear stiffness of airbags by employing a structural dynamics framework, based on Lagrange's equation. This is given by:

$$\frac{d}{dt}\left(\frac{\partial K}{\partial \dot{q}}\right) - \frac{\partial K}{\partial q} + \frac{\partial V}{\partial q} + \frac{\partial D}{\partial \dot{q}} = \frac{\partial W}{\partial q} \tag{8}$$

Where K is the kinetic energy, V is the elastic potential energy, D is the damping on the system, W is the work done on the system, q is a generalized coordinate, and t is a measure of time.

Specifically, a two-degree of freedom model was developed, capturing the system vertical displacement and pitch angle. The choice of these was based on the fact that only the stiffness properties of the airbags in the vertical direction are known, hence limiting the ability to model the system in the lateral degrees of freedom. Even though this is the case, however, these two degrees of freedom capture all the dynamics of interest as they correspond to the Brinkley x-direction – the direction in which the injury-risk criteria are most difficult to meet. Figure 13 presents an idealized three-airbag representation of the modeled system.

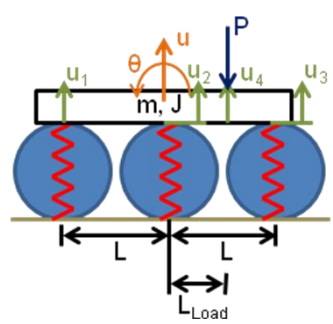

Figure 13. Two Degree of Freedom Multi-Airbag Model

Using Lagrange's equation, the resulting system equations for this particular three airbag system are found to be:

$$\begin{bmatrix} m & 0 \\ 0 & J \end{bmatrix}\begin{bmatrix} \ddot{u} \\ \ddot{\theta} \end{bmatrix} + \begin{bmatrix} k_1 & k_2 & k_3 \\ -Lk_1\cos\theta & 0 & Lk_3\cos\theta \end{bmatrix}\begin{bmatrix} u_1 \\ u_2 \\ u_3 \end{bmatrix} = mg\begin{bmatrix} 1 \\ L_{Load}\cos\theta \end{bmatrix} \tag{9}$$

Where u is the system vertical displacement, θ is the system pitch angle, u_i and k_i are respectively the vertical displacement and non-linear stiffnesses of airbag i, P is the system weight force located at its center of gravity, L is the distance between adjacent airbags, L_{Load} is the distance between the center of gravity and the geometric center of the system, m is the system mass, and J is its mass moment of inertia.

To facilitate the design process, the multi-airbag model was structured such that the user would input only the impact initial conditions and an airbag sizing and configuration combination. From this, the system equations were automatically derived using Lagrange's equation, and solved using a finite difference scheme to obtain the resulting Brinkley response. Note that the full derivation of the underlying equations used in this model can be found in Ref 7.

V. Personal Airbag System Configuration Design and Sizing

Using the multi-airbag model, the configuration of the personal airbag system was designed and sized. Here, the objective was to design a system capable of maintaining the Brinkley DRI to within low injury risk limits during land-landings at the Orion nominal impact velocity of 7.62m/s (25fps)[13], and at impact angles of both 0° and 30° pitch forward. These impact angles were chosen based on an earlier NESC finding that flatter impact angles are preferable for land-landings[2], and that Orion is currently planned for a nominal 30° impact angle. Moreover, further constraints were added to limit the design space. These are summarized in the following problem formulation:

$$Minimize\ \ J(x) = \left[\max(Brinkley\ DRx) \quad \max(Brinkley\ DRz)\right]^T$$

Where:

$$x = Design\ Vector = \begin{bmatrix} Number\ of\ Airbags\,(N) \\ Airbag\ Radius\,(R) \\ Airbag\ Length\,(L) \\ Valve\ Burst\ Pressure\,(\Delta P_{burst}) \\ Orifice\ Area\,(A) \end{bmatrix}$$

Subject to:

$2R(N-1) \leq 1.5m$	**Geometric Constraint** Prevents geometric interference between airbags on the system. 1.5m corresponds to the height of the crash test dummy used for testing when seated in the semi-supine position. See Ref. 7 for details regarding the choice of this position.	(10)
$R_i = R$ $L_i = L$ $A_i = A$	**Commonality Constraints** Improves system robustness and eases manufacture	
$P_{bagI,I} = 102\text{kPa}$	**Fixed Inflation Pressure** Determined from experimental experience during the Single Airbag Drop Test Campaign	
$\sigma = max(P_{bag}(X))R/t < 540MPa$	**Hoop Stress Constraint** Ensures that airbag does not rupture during impact. The rpper bound was determined from material tensile strength tests performed during the Second Development Spiral	

From preliminary executions of the multi-airbag model, it was found that the system experienced a significantly higher injury-risk at impact angles of 30° when compared to those at 0°. As a consequence, this design effort was focused primarily on sizing a system to meet its performance objectives when subjected to a 30° impact angle. Any system which performed adequately under this impact condition would easily meet the injury-risk requirements under a 0° impact condition.

Thus, in order to find a solution to this design problem, a two stage full factorial based methodology was employed to determine the "optimal" solution. This involved firstly performing a coarse resolution full factorial expansion over the design space to filter out regions which experienced either bottoming out or hoop stresses which exceeded the limiting value of 540MPa. When a feasible bounding region was found, a second, high resolution full factorial analysis was performed. From this, the resulting objective space was visualized, and the hoop stress criterion again used to filter out infeasible designs. This was required as it was found that stress infeasible designs were still able to pass the first phase due to the coarse resolution used. Hence, with the resulting feasible set of designs obtained, the minimum Brinkley DRI design was evaluated and if necessary, a decision to modify the configuration concept was made. In total, this optimization process was iterated through three times, with each cycle exploring a unique airbag and valve configuration. The decisions that were made throughout this process are summarized below.

	Configuration	Objective Space
Iteration 1	**Conventional Configuration** Based on the personal airbag system conceptualized during the original NESC workshop. Consists of a row of cylindrical airbags aligned in the longitudinal axis of the seat structure 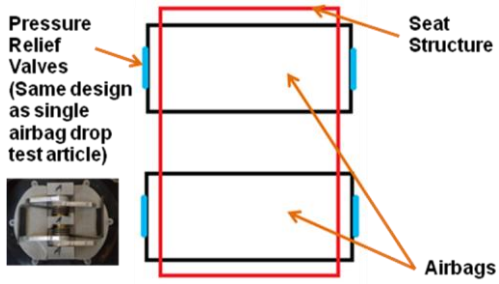 	Entire objective space shown 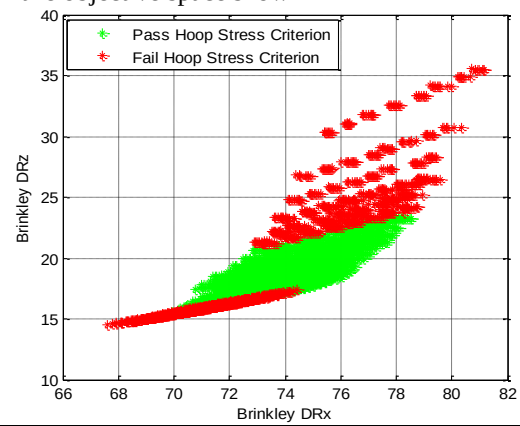
	Observations and Conclusion Even when ignoring the hoop stress criterion, the best performing design has an x-direction Brinkley DRI of 67.59 – a value which far exceeds the limiting value of 28. A drastic configuration change is therefore required	
Iteration 2	**Split-Bag 1-Sided Venting Configuration** Based on findings made in Section IV-D., the intent here is to halve the volume of the airbags by splitting the previous iteration's airbags into two. Moreover, the venting area of each airbag was quadrupled 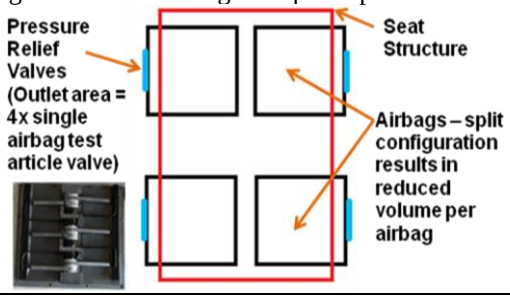 	Objective space filtered by hoop stress criterion and colored by airbag longitudinal length shown 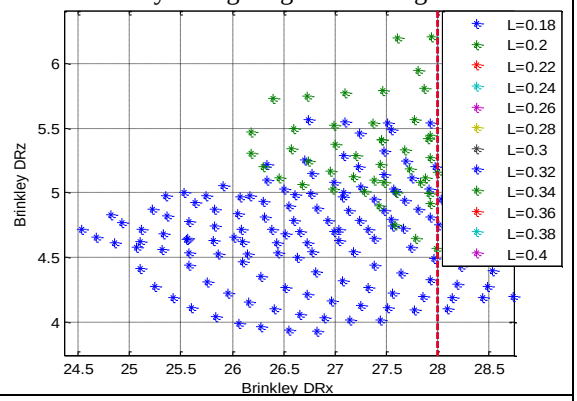
	Observations and Conclusion Several designs meet both hoop stress and injury-risk criteria, however all designs have large aspect ratios (largest airbag axial length of 0.2m, with airbag radii ranging from 0.32-0.34m). These are highly susceptible to local buckling during impact, which in turn has implications on system stability during impact.	
Iteration 3	**Split-Bag 2-Sided Venting Configuration** Concept doubles the venting area on each airbag to further improve impact attenuation capability. This decision was based on the findings discussed in Section IV-D. 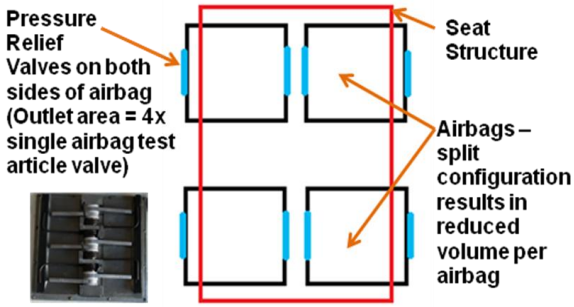 	Objective space filtered by hoop stress criterion and colored by airbag longitudinal length shown 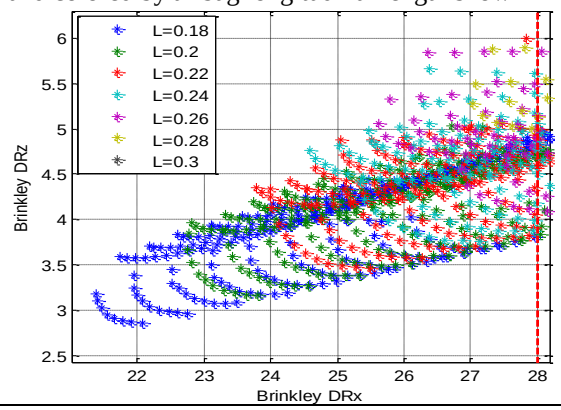

	Summary and Conclusions The maximum airbag length from the set of hoop stress and injury-risk feasible designs increased to 0.28m (with the same airbag radii range of 0.32-0.34m). Lengths in the vicinity of this value were deemed appropriate for maintaining adequate impact stability. Hence, this general configuration was baselined.

With the general system configuration baselined, the specific number of airbags in the longitudinal direction and the final geometry of the bags were finalized by further constraining the generated design space. Here, a seam stress criterion was introduced in order to prevent the airbags from rupturing at the seams during impact. Specifically, an upper bound of 90MPa was set, based on previously conducted tensile strength tests. The combined result of applying all of the abovementioned filters on the objective space is presented below:

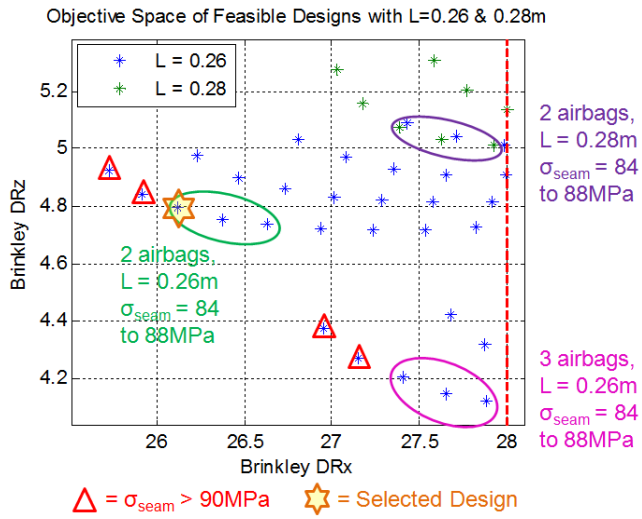

Figure 13. Objective Space Filtered by Max Hoop Stress < 540MPa & L = 0.26m or 0.28m

Table 3 - Final Personal Airbag System Configuration

Design Variable	Value
Airbag Configuration	Split Bag 2-sided Venting
Number of Airbags	2
Valve Type	Pressure relief valve with 4x area of single airbag drop test article
Valve Burst Pressure	8kPa
Airbag Radius	0.32m
Airbag Length	0.26m
Airbag Inflation Pressure	102kPa
Predicted Peak X-Direction Brinkley	16.6 (0° Impact Angle) 26.1 (30° Impact Angle)
Predicted Peak X-Direction Acceleration	11.8Gs (0° Impact Angle) 18.0Gs (30° Impact Angle)

Here, it can be seen that with a higher airbag length of 0.28m, the Brinkley performance moves very close to the low injury-risk limit when compared to the 0.26m length case. It can be further observed that the additional system stiffness of the three-airbag configurations also increases the x-direction Brinkley Index from the two-airbag case by a comparable amount. Moreover, the seam stress criterion was found to have made four of the originally non-dominated designs infeasible, thus limiting the final choice of the system configuration to the set of designs encircled by the green ellipse. From this set, the design with the lowest x-direction Brinkley Index was chosen due to the substantially higher difficulty in meeting the injury-risk criteria in the x-direction, compared to that of the z-direction. This design is highlighted by the yellow star in Figure 13, while its characteristics and predicted performance are respectively summarized in Table 3 and Figure 14.

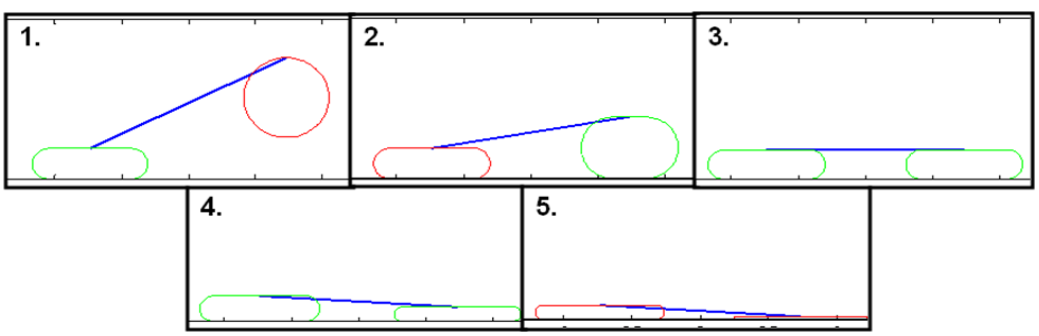

Figure 14. Predicted System Dynamic for the Nominal 30° Impact Case (Red = Valve Closed, Green = Valve Open)

VI. Personal Airbag System Development and Test Plan

With a final design for the personal airbag system established, the development moved into a focused build and integration phase. The result of this was a system which weighed 24% less than the equivalent baseline Orion crew impact attenuation system without any mass optimization purposefully implemented into the system design (See Table A-1 in the Appendix for a detailed mass comparison of the two systems). With the drop test article complete, and proper integration with the purpose-built drop test rig verified; a test plan was developed to achieve the ultimate project objective of determining the feasibility of the personal airbag system concept. Specifically, this plan involved performing two test sessions, each corresponding to drop tests at impact angles of 0° and 30°. During each session, drop tests would be performed from heights of 1 to 10 feet in 1 foot increments. At each height, a minimum of two drop tests would be performed to ensure repeatability of the obtained data. After the second drop at a given height was performed, a preliminary analysis of the results would be performed to determine whether or not a third drop was required to ensure repeatability. Here, the drop height would be measured from the lowest point on the simulated spacecraft floor. Figure 15 shows the final, integrated personal airbag system, as well as the drop configuration for each of the two test sessions.

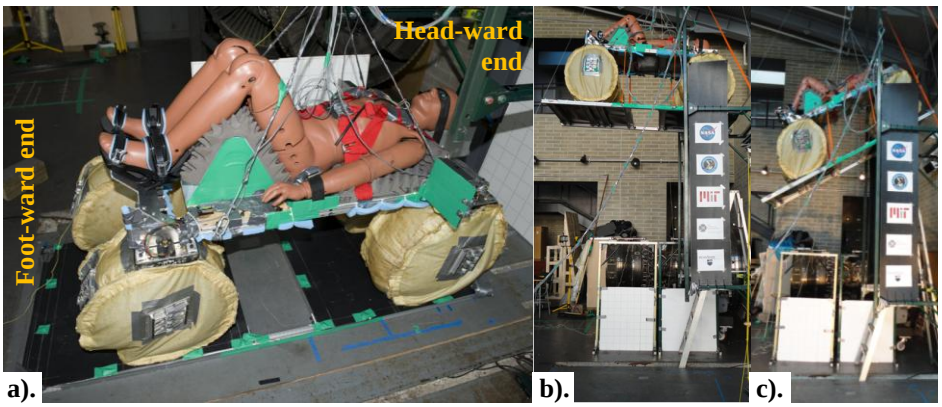

Figure 15. a). Fully Integrated Second Generation Personal Airbag System Drop Test Configuration b). Test Session 1 - 0° Impact Angle c). Test Session 2 - 30° Impact Angle

With regard to data acquisition, a combination of accelerometers, pressure transducers, and high speed camera footage was used. In particular, a set of three tri-axial accelerometers embedded in the chest of a crash test dummy were used to evaluate the Brinkley response, while two perpendicularly separated high speed cameras were used to track LEDs installed about the system. This footage was post processed using photogrammetric analysis techniques to extract transient dynamics data. In addition, pressure transducers were installed on each airbag, enabling for valve performance to be observed, as well as providing a supplementary data set for time synchronization purposes.

VII. Test Results and Analysis

Throughout the month of August 2010, the final drop test campaign was conducted; with a total of 38 drop tests successfully performed. Here, the first test session was successfully completed with a maximum impact velocity of 7.85m/s achieved – a value higher than that anticipated during the nominal 7.62m/s landing of the Orion CEV. The second test session, however, was abruptly ended when a drop height of 7 feet was reached. During this drop, a significant tear was found at the lower hardpoint-to-fabric interface on one of the airbags. Closer inspection of the airbag and corresponding high speed camera footage indicated that, like all failures observed in previous drop test campaigns, this was a result of the formation of a local stress concentration. In particular, this was due to a shearing effect induced on the airbag as the seat structure slid forward relative to the simulated floor during the inclined impact. Although this failure led to an early conclusion to the drop test campaign, a sufficient data set had been obtained to determine system feasibility. The following sections present a detailed analysis of the system impact attenuation performance during both test sessions.

A. Test Session 1 Results (0° Impact Angle)

Figure 16 shows the injury-risk results obtained from all Session 1 drop tests, while Table A-2 in the Appendix provides a summary of this data.

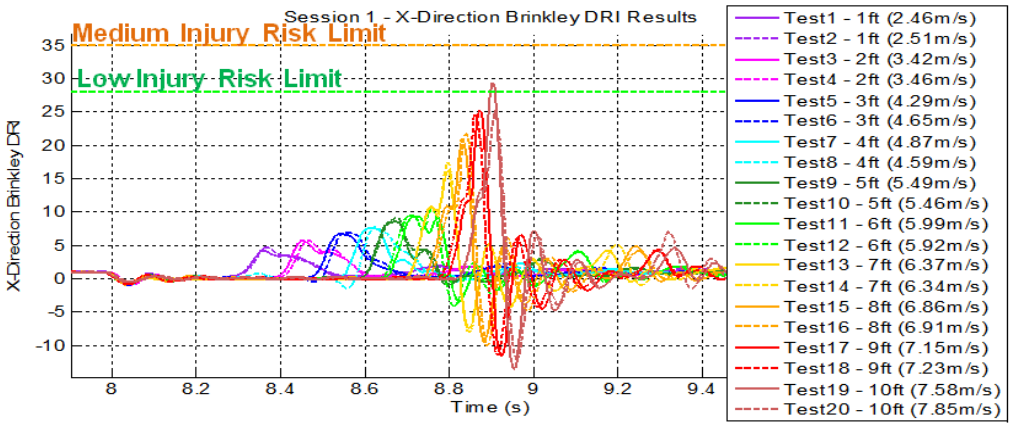

Figure 16. Test Session 1 X-Direction Brinkley DRI Results

Here, it can be seen that at the 10 foot drop height, one of the drops remained within the low-injury risk limit while the other exceeded it. Interestingly, the drop test with the higher impact velocity of 7.85m/s met the safety requirements, whereas the 7.58m/s drop failed to meet them. Since the nominal impact velocity of the Orion MPCV is 7.62m/s (25fps)[13], this suggests that at a 0° impact angle, the system is at the limit of its impact attenuation performance in terms of meeting injury risk requirements for nominal landings. Moreover, because the system was designed to prove concept feasibility, any improvement in performance resulting from more rigorous design and analysis, should produce a system which consistently meets all Brinkley criteria under nominal, non-inclined landings conditions. As a result, it can be definitively stated that:

The airbag-based crew impact attenuation concept is feasible

In addition to this preliminary analysis, a more detailed investigation was conducted to determine why the as-built system had only just met the Brinkley low-injury risk criteria during the 0° impact case, when the predictions made during the design process indicated that it should have easily met the safety requirements (See Table 3). Here, this study focused on Test 19 – the only 0° degree drop test to exceed the low injury-risk limits.

In order to study the mechanics governing this impact case, all obtained data was time synchronized and over-plotted to observe the interactions between the measured properties. This in turn allowed dynamic events of interest to be mapped to the resulting x-direction acceleration profile. The result of this is shown below, in Fig. 17.

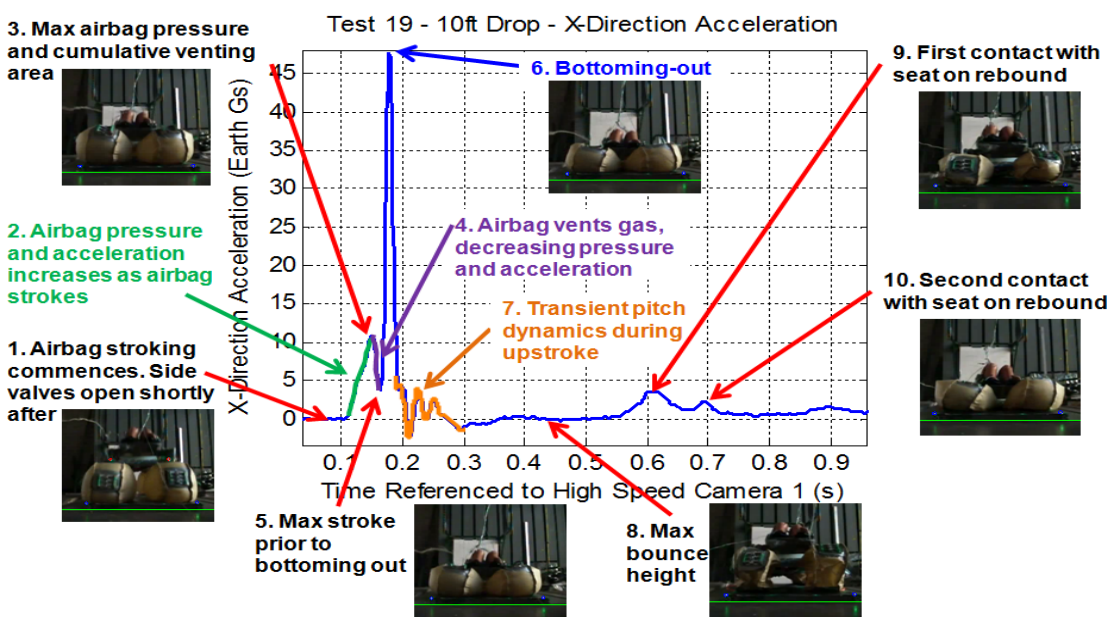

Figure 17. Session 1 Test 19 Dynamically Tagged X-Direction Acceleration Response

Here, it can be seen that the side valves open shortly after the airbags begin to stroke. When the cumulative total area of the valves reaches its peak, the system reaches its first acceleration peak. This suggests that as the airbags stroke and the pressure relief valves open, the acceleration and corresponding pressure increases until the peak opening area is achieved. At this moment, the effect of the gas vented from the airbags causes the experienced acceleration to decrease. As this occurs, the airbag continues to stroke until either the system comes to rest or the stroke is depleted, causing a bottoming-out event to occur. For this particular case, the latter scenario was experienced, causing a subsequent sharp acceleration spike. Here, the correlation between this spike and a bottoming event was verified using high speed camera footage.

Following this bottoming-out event, the system was found to experience transient pitch dynamics as it bounced off the ground surface. After reaching its maximum bounce height, the system experienced a second impact with the ground, registering two miniature peaks in the acceleration response as various parts of the system came into contact with the ground surface.

Using this newly obtained insight, the entire Test Session 1 data set was revisited in an attempt to gain additional insight into the system performance. From this, it was found that the system dynamics is a superposition of the natural airbag dynamics, and the dynamics of bottoming-out. Specifically, this refers to the natural functions of airbag compression, pressure build-up, and venting characterized by the first peak observed in the acceleration response; and the bottoming-out dynamics characterized by the acceleration spike occurring shortly thereafter. This suggests that if this bottoming-out dynamics can be prevented, the overall system performance can be vastly improved due to the consequent reduction in peak acceleration and corresponding Brinkley Index. This can be seen in Fig. 18, where the peak acceleration for the 10 -=foot drop case would be 12.6G's, if bottoming-out is prevented. Interestingly, this potential peak acceleration is very close to the 11.8G peak acceleration value predicted by the multi-airbag model for 0° impact case. In regards to the corresponding injury-risk, this equates to a reduction in the peak Brinkley DRI value by a factor of at least 2, based on the stiffness and damping ratio values of the Brinkley model in the x-direction.

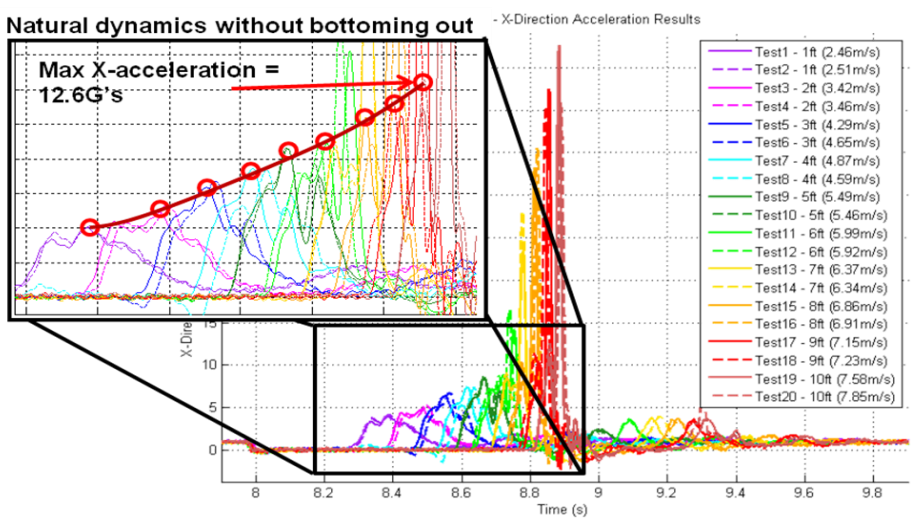

Figure 18. Potential System Dynamics without Bottoming-Out

From a practical point of view, this motivates the need to explore the implementation of anti-bottoming airbags within the system, an additional airbag whose purpose is to prevent direct contact between the payload mass and the impacting surface. Typically installed in a "bag within a bag" configuration, it is hypothesized that by adding anti-bottoming airbags, the influence bottoming-out on the overall system dynamics will be largely mitigated. Figure 19 shows one such example of this concept.

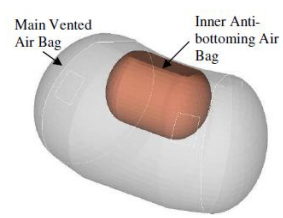

Figure 19. Anti-Bottoming Airbag Concept[14]

B. Test Session 2 Results (30° Impact Angle)

In order to quantify and analyze the multi-airbag system performance during the second test session, the same approach as that employed for the first test session was used. Figure 20 presents the injury-risk data obtained for all Session 2 drop tests, while Table A-3 in the Appendix summarizes the entire dataset obtained. Note here that three drop tests were performed at heights of 3 and 6 feet due to inconsistencies observed in the dataset after the second drop.

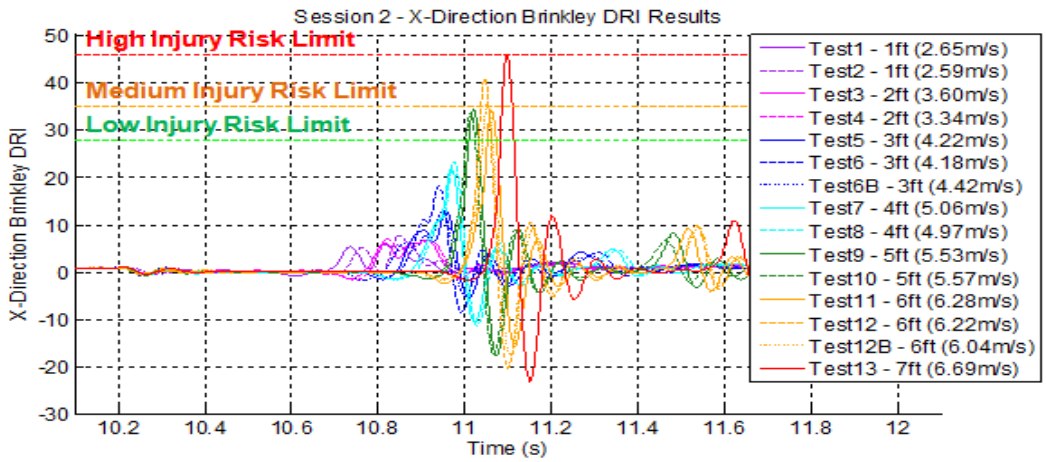

Figure 20. Test Session 2 X-Direction Brinkley DRI Results

Here, it can be immediately seen that the system does not perform adequately during 30° impact angles, with the low-injury risk criteria being exceeded at drop heights of 5 feet, the medium injury-risk criteria being exceeded at drop heights of 6 feet, and the high injury-risk criteria being exceeded during the failed drop tests at 7 feet. Considering the fact that all of these failed drops had impact velocities less than the nominal 7.62m/s, this result definitively verifies the original NESC finding that flatter angles are more favorable for land-landings.

As a consequence of this finding, a study was initiated to determine the reasons as to why the system performed so poorly at the 30° impact angle. Here, the same process as that used in the detailed analysis of the Test Session 1 results was employed, whereby all data sources were time synchronized and over-plotted to investigate their interactions. In addition to this, a line detection scheme was also implemented to enable the extraction of attitude information from the high speed camera footage. This data was primarily used to predict the moment of impact of the front edge of the simulated floor, thereby allowing for the high speed camera footage to be time synchronized with other data sources. For this particular study, the worst performing test case was chosen as the baseline, being the single drop performed from 7 feet. Figure 21 summarizes the results of this analysis.

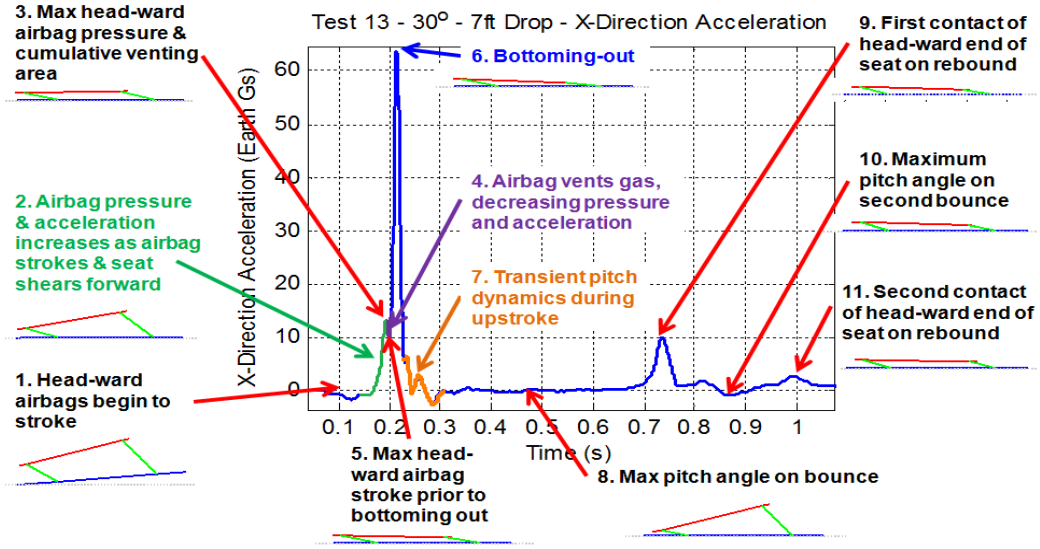

Figure 21. Session 2 Test 13 - Dynamically Tagged X-Direction Acceleration Response with Resimulated Dynamics shown underneath each tag (Red line = Seat, Blue line = Simulated spacecraft floor, Green line = Vector connecting airbag attachment points on system

From Fig. 21, it can be seen that shortly after the first acceleration peak, the system experiences a bottoming out event, as observed in the first test session results. Here, the short period of decreasing acceleration between the first and second acceleration spikes indicates that there was significantly less stroke in the airbags prior to bottoming-out, when compared to the 0° impact case. Again, following this bottoming-out event, the system experiences the

previously observed transient pitch dynamics during its rebound, after which it obtains a maximum pitch angle during the peak height of its bounce. In turn, this pitch angle causes the system to experience a second impact at an inclined angle.

Upon comparison of the dynamically tagged acceleration response with the high speed camera footage, it was noticed that all peak acceleration events occurred as a result of the head-ward end (refer to Fig. 15a)) of the seat pivoting about the foot-ward airbags. Closer inspection of the video footage captured during this test indicated that this was a result of the differential stroking of the foot-ward and head-ward airbags, causing the head-ward end of the seat to pivot about the feet and towards the ground as it continued to fall. As the seat pivoted about the foot-ward airbags, it sheared forward relative to the simulated floor, hence removing a significant amount of stroke from the head-ward airbags. This hence explains the short decrease in acceleration between the first and second acceleration peaks observed in Figure 21. Furthermore, by the time the head-ward airbags began to stroke, most of the air in the foot-ward airbags had already been depleted, causing this foot-ward end to continue to act as a pivot point for consequent rebounds of the system. These events can be seen in the original frame by frame breakdown of this drop test, presented in Fig. 22.

Here, the presence of this shearing effect suggests that the three row configuration found on the Pareto front shown in Fig. 13, may have been preferable in the design of the airbag configuration. The inclusion of an additional row of airbags between the existing airbags could potentially compensate for the lost stroke in the head-ward airbags due to the forward shearing motion. In turn, this would increase the time over which the acceleration response decreases after the first peak, thereby reducing the magnitude of any subsequent bottoming-out event.

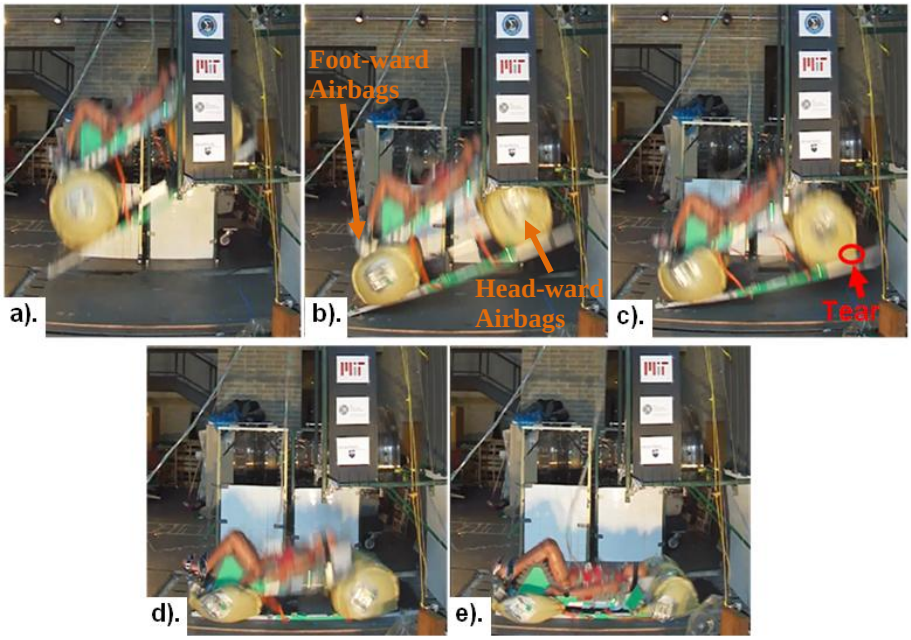

Figure 22. Frame by Frame Breakdown of the 7 foot, 30° Impact Angle Drop a). System in free-fall b). Differential Stroking between Foot-ward and Head-ward Airbags as system makes first contact with ground surface c). Forward Shearing of Seat System relative to Simulated Floor. Also shown here is the location of the tear experienced during this drop d). Start of Head-ward Airbag Stroke. Note that a significant amount of stroke from these airbags has been removed due to the forward shearing of the Seat System. Additionally, most of the air in the Foot-ward airbags has been depleted by this point, causing them to act as a pivot point e). System Rest after multiple impacts of the Head-ward end of the seat with the ground surface

VIII. Conclusion

A full scale personal airbag system was designed, developed and subjected to an extensive drop test campaign in an attempt to investigate its impact attenuation performance, and in turn, the feasibility of the airbag-based crew impact attenuation concept. Through this effort, this concept has been proven to be feasible. This feasibility is further verified by the fact that all drop tests were performed on land, with the only means of impact attenuation

being the airbag system. This contrasts significantly to the more benign nominal Orion landing scenario of water landings attenuated by both crushable structures and strut-based mechanical damping. Moreover, the fact that the final developed system met these objectives while being 24% lighter than the baseline Orion system; provides further support for airbag-based crew impact attenuation, especially given the fact that no mass optimization was actively performed on the design of the seat structure used to support the occupant.

Additionally, this study has yielded two key insights into the performance of the personal airbag system. The first of which, is that the dynamic response of the system during impact is a superposition of the natural airbag dynamics and the dynamics of bottoming-out. By mitigating the effects of bottoming-out, it was found that the resulting peak Brinkley response under nominal landing conditions could be more than halved. This in turn motivates the need to explore the implementation of anti-bottoming airbags into the system.

The second important insight gained from this effort is related to the reasons as to why inclined impacts resulted in significantly poorer performance compared to impacts at flatter angles. Here, it was found that this was due to a combination of differential stroking between the front and rear airbags, and a consequent forward shearing motion between the seat and the simulated floor. The resultant effect of this was the removal of a significant amount of stroke from the head-ward airbags, and pivoting of the system about the foot-ward airbags causing further impacts of the head-ward end of the system. Moreover, the presence of the observed shearing effect motivates the need to revisit the design of the airbag configuration, where the inclusion of an additional row of airbags may potentially offset the adverse effects of this shearing motion.

With regard to the implementation of airbag-based crew impact attenuation aboard the Orion MPCV and other future spacecraft, these findings have both upstream and downstream implications on the spacecraft design. These include the impact angle, and hence the hang angle of the spacecraft underneath its parachutes; as well as the configuration of the crew cabin, where variables such as the cabin geometry, crew relative positioning constraints relative to the spacecraft controls and viewing ports, and stowage constraints, will interact with the design of the airbag-based system. Although the feasibility of a personal airbag-type system meeting all of these design specific constraints is yet to be determined, this study has proven that this concept is capable of performing the fundamental function of protecting astronauts from the impact loads incurred during land-landings, with a lower mass penalty than current systems. This finding hence warrants the inclusion of this airbag-based crew impact attenuation in the Earth landing system tradespace of Orion, and future spacecraft.

Appendix

Presented below is a mass comparison between the baseline Orion Crew Impact Attenuation System, and the personal airbag system. Here, the mass values for the Orion system were provided by the project sponsor.

Table A-1 – Mass Comparison between the baseline Orion Crew Impact Attenuation System and the Personal Airbag System

Orion Crew Impact Attenuation System	
Component	**Mass**
Crew Seats	
Operators 1 & 2	31.3kg (69lb) each
Operators 3-6	27.4kg (60.5lb) each
System Support Structure	
Pallet Struts (9 total: 4-X, 3-Y, 2-Z)	10.9kg (24lb) each (average)
Miscellaneous components supported by system	100kg (221lb)
Total Mass	**493.5kg (1088lb)**

Generation 2 Personal Airbag System	
Component	**Mass**
Crew Seats (6 total)	27.7kg (61lb) each
System Support Structure	
Integrated Airbag (4 per crew member)	4.0kg (8.8lb) each
Inflation System	11.3kg (25lb)
Miscellaneous components supported by system	100kg (221lb)
Total Mass	**373kg (823lb)**

Presented below is a summary of all successfully drop tests performed with the personal airbag system:

Table A-2 – Summary of Personal Airbag System Drop Test Session 1 (0° Impact Angle) Results

Test No.	Drop Height (ft)	Impact Velocity (m/s)	Max X-Acceleration (G's)	Max Brinkley DRx	Max β-Number
1	1	2.46	4.004	4.23	0.152
2	1	2.51	4.128	4.71	0.170
3	2	3.42	4.923	5.77	0.207
4	2	3.46	5.302	5.77	0.210
5	3	4.29	6.356	6.73	0.241
6	3	4.65	6.689	6.90	0.252
7	4	4.87	7.427	7.59	0.272
8	4	4.59	7.384	7.70	0.293
9	5	5.49	8.575	8.57	0.308
10	5	5.46	8.643	9.12	0.328
11	6	N/A	14.208	9.42	0.340
12	6	5.92	16.562	10.51	0.376
13	7	6.37	23.444	16.10	0.606
14	7	6.34	28.068	17.38	0.634
15	8	6.86	33.178	20.95	0.770
16	8	N/A	35.472	21.73	0.809
17	9	7.15	42.474	25.28	0.934
18	9	7.23	40.451	24.70	0.919
19	10	7.58	47.544	29.46	1.083
20	10	7.85	40.298	25.09	0.944

NB. "N/A" implies that the high speed camera footage captured did not provide enough information to extract the stated variable.

Table A-3 – Summary of Personal Airbag System Drop Test Session 2 (30° Impact Angle) Results

Test No.	Drop Height (ft)	Impact Velocity (m/s)	Max X-Acceleration (G's)	Max Brinkley DRx	Max β-Number
1	1	2.65	6.714	5.79	0.298
2	1	2.59	7.277	7.75	0.290
3	2	3.6	8.089	6.84	0.300
4	2	3.34	7.986	6.97	0.300
5	3	4.22	17.428	12.91	0.510
6	3	4.18	27.897	18.05	0.711
6B	3	4.42	17.476	13.27	0.504
7	4	5.06	32.353	21.83	0.818
8	4	4.97	36.103	23.22	0.868
9	5	5.53	47.274	34.45	1.237
10	5	5.57	46.522	33.65	1.217
11	6	6.28	53.321	33.95	1.237
12	6	6.22	53.359	40.79	1.466
12B	6	6.04	48.074	35.25	1.263
13	7	6.69	63.754	45.91	1.642

Acknowledgments

Financial support for this research was provided by the NASA Engineering Safety Center (NESC) and the Constellation University Institutes Program (CUIP) under prime award number NCC3989 and subaward Z634013. The authors would like to thank Joe Pellicciotti, Tim Brady, Charlie Camarda, Chuck Lawrence, Cory Powell and Ed Fasanella of the NESC for their technical support of this work; as well as Lisa Jones and her team at NASA LaRC for their assistance with the loan of a Hybrid II crash test dummy. Many thanks also go to Todd Billings, Dave Robertson, and Dick Perdichizzi of the MIT Department of Aeronautics and Astronautics for their invaluable contribution to the manufacturing and integration of the hardware developed throughout this project.

References

[1]Johnson, C.J. and Hixson, R.A., "Orion Vehicle Descent, Landing, and Recovery System Level Trades," AIAA 2008-7745

[2]Baker, J.D., Eisenman, D.J, Yucknovicz, D.E., "Evaluation of Land versus Water Landings for Crew Exploration Vehicle," NASA Document RP-07-29

[3]Davis, C.E.J., and Jahn, N.P., "Qualification Test of Apollo Crew Couch X-X Axis Foot Cyclic Impact Strut Assembly (V36-571711-121)," North American Rockwell Corporation, NA-68-474, January 1969, Los Angeles, CA.

[4]de Weck, O.L, "Personal Airbag System – NASA NESC Research Project Overview," Presentation to NESC Orion Alternative Seat Attenuation Systems Team, March 17 2009

[5]Do, S., de Weck, O.L., Robles Jr., R., Pellicciotti, J., and Brady, T., "An Airbag-Based Crew Impact Attenuation System Concept for the Orion CEV – First Generation System Development," AIAA 2009-6438

[6]Boehm, B. W., "A Spiral Model of Software Development and Enhancement," Computer, May 1988, pp. 61-72.

[7]Do, S., "An Airbag-Based Crew Impact Attenuation System for the Orion Crew Exploration Vehicle," S.M. Dissertation, Dept. of Aeronautics and Astronautics, Massachusetts Institute of Technology, Cambridge, MA, 2011.

[8]NASA Constellation Program Human-Systems Integration Requirements, CxP 70024, Released 15 December, 2006

[9]Lawrence, C., Fasanella, E.L., Tabiei, A., Brinkley, J.W., and Shemwell, D.M., "The Use of a Vehicle Acceleration Exposure Limit Model and a Finite Element Crash test Dummy Model to Evaluate the Risk of Injuries During Orion Crew Module Landings," NASA TM-2008-215198

[10]Cole, J.K. and Waye, D.E., "BAG: A Code for Predicting the Performance of a Gas Bag Impact Attenuation System for the PATHFINDER Lander," SAND93-2133, November 1993

[11]Esgar, J.B., and Morgan, W.C., "Analytical Study of Soft Landings on Gas-Filled Bags," NASA Technical Report R-75, Lewis Research Center, Cleveland, Ohio, 1960

[12]Cengal, Y.A., and Turner, R.H., "Fundamentals of Thermal-Fluid Sciences," McGraw-Hill Companies, 2005, Boston, pg. 1111.

[13]Lawrence, C., Carney, K.S., and Littell, J., "Astronaut Risk Levels During Crew Module (CM) Land Landing," NASA GRC, NASA-TM-2007-214669, Cleveland, OH.

[14]Timmers, R.B., Hardy, R.C., Willey, C.E., and Welch, J.V., "Modeling and Simulation of the Second-Generation Orion Crew Module Air Bag Landing System," AIAA 2009-6593